Hourly Coordination of Electric Vehicle Operation and Volatile Wind Power Generation in SCUC

Mohammad E. Khodayar, *Student Member, IEEE*, Lei Wu, *Member, IEEE*, and Mohammad Shahidehpour, *Fellow, IEEE*

***Abstract*—In this paper, the coordinated integration of aggregated plug-in electric vehicle (PEV) fleets and renewable energy sources (wind energy) in power systems is studied by stochastic security-constrained unit commitment (Stochastic SCUC) model, which minimizes the expected grid operation cost while considering the random behavior of the many PEVs. PEVs are mobile and distributed devices with deferrable options for the supply/utilization of energy at various times and locations. The increased utilization of PEVs, which consume electricity rather than fossil fuel for driving, offers unique economic and environmental opportunities, and brings out new challenges to electric power system operation and planning. The storage capability of PEVs could help power systems mitigate the variability of renewable energy sources and reduce grid operation costs. Vehicle-to-grid (V2G) enables PEVs to have bi-directional power flows once they are connected to the grid, i.e., they can either inject power to, and draw power from, the grid which adds further complexity to power system operations. PEVs signify customers' random behavior when considering their driving patterns, locational energy requirements, topological grid interconnections, and other constraints imposed by the consumers. Numerical tests demonstrate the effectiveness of the proposed approach for analyzing the impact of PEVs on the grid operation cost and hourly wind energy dispatch.**

***Index Terms*—Load aggregation, plug-in electric vehicles, renewable energy sources, stochastic security-constrained unit commitment, V2G.**

NOMENCLATURE

Variables:

b, j, o	Index of bus.
$C_{(.)}^{(.)}$	Operation cost of PEV fleet.
$E_{v,t}^{(.)}$	Available energy in batteries of fleet v at time t.
$E_{v,t}^{net}$	Net discharged energy of PEV fleet v at time t.
$F_{c,(.)}, F_{c,(.)}^{r}$	Production/availability cost function of a thermal unit.
i	Denotes a thermal unit.
$I_{(.)}^{(.)}$	Unit status indicator, 1 means on and 0 means off.
$I_{c,(.)}^{(.)}$	Indicator of PEV fleet in charging mode.
$I_{dc,(.)}^{(.)}$	Indicator of PEV fleet in discharging mode.
$I_{i,(.)}^{(.)}$	Indicator of PEV fleet in idle mode.
k	Denotes a hydro unit.
l	Index of transmission line.
m	Denotes a segment of curves.
$P_{(.)}^{(.)}$	Generation of a unit.
$P_{d,w,t}^{(.)}$	Power generation curtailed of wind unit w at hour t.
$P_{c,(.)}^{(.)}, P_{dc,(.)}^{(.)}$	Charge/discharge power of PEV fleet.
$P_{m,(.)}^{(.)}$	Charge/discharge power rate at segment m.
$PL_{l,t}^{(.)}$	Real power flow on line l at hour t.
s	Denotes a scenario.
$SD_{(.)}^{(.)}$	Shutdown cost of a unit.
$SU_{(.)}^{(.)}$	Startup cost of a unit.
t	Hour index.
v	Denotes a PEV fleet.
w	Denotes a wind unit.
$\theta_{(.)}^{(.)}$	Bus angle.
$\Delta_{(.)}^{\max}$	Maximum permissible power adjustment of a unit.

Constants:

$B_{b,t}^{(.)}$	Set of units which are connected to bus b at time t.
$b_{m,(.)}$	Slope of segment m in linearized charge/discharge curve.
CD_k, CS_k	Shutdown/startup cost of hydro unit k.
D_b	Set of loads which are connected to bus b.
$DR_{v,t}^{s}$	Energy for PEV v to drive at time t in scenario s.
$E_v^{\min}, E_v^{\max}$	Min/max energy stored in batteries of PEV fleet v.
$E0_v, ET_v$	Initial and terminal stored energy in PEV fleet v.
$L_{f,b}, L_{t,b}$	Set of lines starting from/ending at bus b.

Manuscript received August 03, 2011; revised November 27, 2011; accepted December 23, 2011. Date of publication June 15, 2012; date of current version August 20, 2012. Paper no. TSG-00317-2011.

M. E. Khodayar and M. Shahidehpour are with the Electrical and Computer Engineering Department, Illinois Institute of Technology, Chicago, IL 60616 USA (e-mail: mkhodaya@iit.edu; ms@iit.edu).

L. Wu is with the Electrical and Computer Engineering Department, Clarkson University, Potsdam, NY 13699 USA (e-mail: lwu@clarkson.edu).

Color versions of one or more of the figures in this paper are available online at http://ieeexplore.ieee.org.

Digital Object Identifier 10.1109/TSG.2012.2186642

$N_{v,t}$	Status of grid connection of fleet v at time t.
NE_v^s	Ratio of the number of PEVs in fleet v in scenario s to the number of base case PEVs.
NT	Number of hours under study.
p^b	Probability of the base case solution.
p^s	Probability of scenario s.
$P_{(.)}^{\min}, P_{(.)}^{\max}$	Min/max generation capacity.
$P_{c,v}^{\min}, P_{c,v}^{\max}$	Min/max charging capacity of PEV fleet v.
$P_{dc,v}^{\min}, P_{dc,v}^{\max}$	Min/max discharging capacity of PEV fleet v.
$P_{D,(.)}^{(.)}$	Total system demand.
$P_{f,w,t}^{(.)}$	Forecasted wind power of wind unit w at hour t.
$P_{m,v}^{\max}$	Maximum power output at segment m in charging/discharging cost curve of PEV fleet v.
$PL_l^{\max}$	Maximum capacity of line l.
$\hat{T}$	Time in which the charging state is set to a value.
$UX_{(.)}^{(.)}, UY_{(.)}^{(.)}$	Outage status, 1 if available, and otherwise 0.
X_{jo}	Inductance of a line between buses j and o.
η_v	Cycle charging efficiency of PEV fleet.

I. Introduction

PLUG-IN electric vehicles (PEVs) represent hourly distributed and mobile demands in power systems which could also provide distributed storage to power grids [1], [2]. The aggregated storage capability of PEVs can help shift the hourly generation portfolio and reduce grid operation costs. Hence, a dramatic increase in the number of PEVs could have a major impact on power system operations. Once aggregated at the distribution level, the distribution company (DISCO) will submit the information on marginal cost, storage capacity, and location of PEV fleets to the ISO for participation in the day-ahead market.

Wind energy is the fastest growing renewable energy resource [3]. The large penetration of wind energy could decrease the operation cost and the emission of hazardous gases from fossil plants. However, the variability of wind energy could impose adverse effects on the dynamic and static security of power systems. References [4] and [5] studied the integration of storage for mitigating the effect of hourly wind energy variability on power systems. Likewise, V2G could offer ancillary services and reduce operation costs in power systems.

References [6]–[8] focused on storage technologies and power electronic grid-connection interfaces for facilitating large-scale adoptions of PEVs. Economic potentials of PEVs for participating in regulation services were investigated in [9]. The role of PEV in the integration of renewable energy resources was addressed in [10]. The integration of PEV in power systems was investigated in [11] and major issues for the V2G implementation were discussed. The electricity market issues of PEV integration were presented in [12].

Unlike conventional storage capabilities, the grid-connection storage topography of PEVs may change during the daily operation of power systems. PEVs consume energy according to their driving requirements. In addition, the total PEV energy drawn from the grid could be much larger than the energy injected to the grid [13]–[16]. While most of the previous studies addressed the economic aspects of integrating PEVs to power systems, they lack the transmission system security consideration offered by the PEV interconnection and its daily profile in power systems.

The contributions of this paper include the modeling of large scale PEV integration as mobile distributed load and storage facilities and their impacts on the optimal operation of security-constrained power systems. The study considers physical limitations of power systems, hourly load and wind energy uncertainties, and random outages of generation and transmission components in PEV integration.

The rest of the paper is as follows. Section II discusses the proposed Stochastic SCUC formulation. Section III illustrates the effectiveness of the proposed methodology by a 6-bus system and the IEEE 118-bus system. Detailed discussions and conclusions are presented in Sections IV and V, respectively.

II. Proposed Stochastic SCUC Formulation

PEV fleet characteristics include starting locations and destinations of PEV fleets, departure and arrival times at designated locations, and PEV charging locations and patterns which could be bundled into power system operations. A random number of PEVs is assumed for each fleet. The state of charge (SOC), energy consumption, and min/max capacity of a PEV fleet is a function of the number of PEVs and their operating characteristics. SOC is the ratio of available energy to maximum storable energy in the battery. The available energy in the PEV battery is computed by multiplying the given SOC by the maximum storable energy in the battery. The energy consumption in a fleet, which is a parameter, depends on the number of PEVs and their energy requirements. The driving habits in a fleet would determine the charging/discharging patterns of aggregated PEVs.

The proposed formulation is a stochastic optimization problem in which the wind energy and load forecast errors, power system component outages, number of PEVs in a fleet and their energy requirements are considered as variables. The proposed solution determines the hourly unit commitment and dispatch of generating units and charge/discharge states of PEV fleets.

The Monte Carlo simulation method is utilized in the proposed stochastic model. Random outages in power systems are represented by incorporating probability distribution functions and forced outage rates. Load forecast errors, PEV energy consumption patterns, and the number of PEVs in a fleet are represented by truncated normal distribution functions in which the mean values are the forecasts and the standard deviations are percentages of the mean values [17], [18]. Wind speed variations are simulated by the Weibull distribution function, auto correlation factor and diurnal pattern [19], and wind generation is procured by incorporating the wind turbine power curve and wind speed at wind sites. Forward and backward algorithms are developed to reduce the number of scenarios with an acceptable accuracy [20], [21]. The convex operation cost of aggregated PEVs would depend on the number of vehicles and charging/discharging cycles [9].

The proposed Stochastic SCUC is a mixed-integer programming (MIP) optimization problem. The objective (1) is to minimize the grid operation cost subject to system and unit constraints (2)–(28). The objective function includes the base case operation cost, in which the forecasted quantities of load, wind, and hydro are incorporated, and outages of generators and transmission lines are not considered. We also consider in the objective function the availability cost for providing spinning reserve in Monte Carlo scenarios. The availability cost refers to the payment to generators that provide reserves. The provision of reserve is exercised as a corrective action by generators in response to the realization of uncertainties. It is assumed that the generators can provide corrective actions, which are restricted by their ramp up/down limitations. The availability cost is considered as one third of the marginal cost of a generating unit [22]. The objective function further includes the expected cost of corrective actions in scenarios for accommodating uncertainties. In this formulation, load curtailment is not acceptable in scenarios, and the system should serve the load in the base case and all scenarios. Alternatively, load curtailment could have been considered by adding the respective penalty factor to the objective function. Thermal units are formulated as non–quick start units, so their scenario commitment status is the same as that in the base case. Thus, there is no need to introduce extra startup/shutdown costs in scenarios.

The system and generating unit constraints in the base case are shown in (2)–(14). Detailed thermal unit constraints are available in [23]. Hydro unit constraints are provided in [24]. Wind curtailment constraint is shown in (2) in which the sum of dispatched and curtailed wind power is the same as the wind power forecast. The wind curtailment occurs when there is an insufficient ramping down capability of thermal units or a significant transmission congestion for utilizing the available wind power in power systems. The base case PEV fleet constraints are shown in (3)–(10). The net hourly absorbed/delivered energy is given in (3), which shows that the difference in the energy gained from the grid/stored in the aggregated PEV battery and the energy delivered back to the grid from the PEV is quantified by the charging cycle efficiency of the aggregated PEV. The hourly charge/discharge/idle modes of fleets which are mutually exclusive are given in (4). Charge/discharge power constraints are given in (5)–(6). The hourly energy balance in PEV batteries is given in (7).The given parameter $N_{v,t}$ indicates connectivity of PEV fleet to the system. Once a PEV fleet is connected to the power system (i.e., $N_{v,t} = 1$), the aggregated battery is either charged by drawing power from the grid (5), or discharged by injecting power to the grid (6). If the PEV fleet is not plugged in (i.e., $N_{v,t} = 0$), the charging/discharging power will be zero according to (4)–(6).The energy capacity limit of each fleet is presented in (8)–(9). The piecewise linear representation of convex charge/discharge cost curve of PEV batteries is shown in (10), which represents the depth of discharge and cycles to failure of the battery for calculating the cost of energy drawn or delivered by PEV batteries. As the depth of aggregated battery discharge increases, the number of cycles to failure would decrease. This indicates a higher cost for charging/discharging of the battery because the total energy stored by/drawn from the battery during its lifetime will decrease for a fixed battery price [9], [11]. Hence, the operation cost of aggregated PEV has a direct correlation with the depth of charging/discharging batteries [12]. The nonlinear battery charging/discharging cost curves are piecewise linearized for consideration in the proposed MIP formulation. A tighter piecewise linear approximation was presented in the authors' previous work [25]. In the consumer-controlled scheme, the aggregated SOC of PEVs is set to be fixed at specific operation periods (11). It is assumed that the SOC is at 100% when a PEV fleet is leaving the station. Equations (12)–(14) represent the base case dc power flow constraints.

The PEV fleet scenario constraints are shown in (15)–(23) and the consumer-controlled scenario scheme is represented by (24). The wind scenario constraint includes a set similar to (2), except base case variables are replaced by scenario variables. The scenario corrective action is enforced by (25) where the hourly cost of corrective action, $F^r_{c,i}(\Delta^{\max}_{i,t})$, is included in (1). Equations (26)–(28) represent dc power flow constraints for each Monte Carlo scenario. The grid connection of PEV fleet at time t is represented by $B^v_{b,t}$ in (26).

$$\text{Min}\begin{bmatrix}\sum_t\sum_i\left(p^b\cdot F_{c,i}(P_{i,t})+SU_{i,t}+SD_{i,t}\right)+\\ \sum_t\sum_k p^b\cdot(SU_{k,t}+SD_{k,t})+\sum_t\sum_v p^b\cdot C_{v,t}\end{bmatrix}+\left[\sum_t\sum_i\left(F^r_{c,i}\left(\Delta^{\max}_{i,t}\right)\right)\right]$$
$$+\sum_s p^s\cdot\left[\sum_t\sum_i F_{c,i}\left(P^s_{i,t}\right)+\sum_t\sum_k\left(SU^s_{k,t}+SD^s_{k,t}\right)+\sum_t\sum_v C^s_{v,t}\right] \tag{1}$$

s.t.

$$P_{w,t}+P_{d,w,t}=P_{f,w,t} \tag{2}$$
$$E^{net}_{v,t}=P_{dc,v,t}-\eta_v\cdot P_{c,v,t} \tag{3}$$
$$P_{v,t}=P_{dc,v,t}-P_{c,v,t}$$
$$I_{dc,v,t}+I_{c,v,t}+I_{i,v,t}=N_{v,t} \tag{4}$$
$$I_{c,v,t}\cdot P^{\min}_{c,v}\le P_{c,v,t}\le I_{c,v,t}\cdot P^{\max}_{c,v} \tag{5}$$
$$I_{dc,v,t}\cdot P^{\min}_{dc,v}\le P_{dc,v,t}\le I_{dc,v,t}\cdot P^{\max}_{dc,v} \tag{6}$$
$$E_{v,t}=E_{v,t-1}-E^{net}_{v,t}-(1-N_{v,t})\cdot DR_{v,t} \tag{7}$$
$$E^{\min}_v\le E_{v,t}\le E^{\max}_v \tag{8}$$
$$E_{v,0}=E_{v,NT} \tag{9}$$
$$C_{v,t}=N_{v,t}\cdot\left(\sum_m b_{m,v}\cdot P_{m,v,t}\right)\quad 0\le P_{m,v,t}\le P^{\max}_{m,v}$$
$$N_{v,t}\cdot\left|E_{v,t}-E_{v,t-1}\right|=\sum_m P_{m,v,t} \tag{10}$$
$$E_{v,\hat{T}}=E^{\max}_v \tag{11}$$
$$\sum_{i\in B^i_b}P_{i,t}+\sum_{w\in B^w_b}P_{w,t}+\sum_{v\in B^v_{b,t}}P_{v,t}+\sum_{k\in B^k_b}P_{k,t}$$
$$=\sum_{d\in D_b}P^d_{D,t}+\sum_{l\in L_{f,b}}PL_{l,t}-\sum_{l\in L_{t,b}}PL_{l,t} \tag{12}$$
$$PL_{l,t}=\frac{(\theta_{j,t}-\theta_{o,t})}{X_{jo}} \tag{13}$$
$$|PL_{l,t}|\le PL^{\max}_l \tag{14}$$

$$C_{v,t}^{s} = N_{v,t} \cdot \left(\sum_{m} b_{m,v} \cdot P_{m,v,t}^{s} \right)$$
$$0 \le P_{m,v,t}^{s} \le P_{m,v}^{\max} \cdot NE_{v}^{s} \tag{15}$$

$$N_{v,t} \cdot \left| E_{v,t}^{s} - E_{v,t-1}^{s} \right| = \sum_{m} P_{m,v,t}^{s}$$
$$E_{v,t}^{net,s} = P_{dc,v,t}^{s} - \eta_{v} \cdot P_{c,v,t}^{s} \tag{16}$$
$$I_{dc,v,t}^{s} + I_{c,v,t}^{s} + I_{i,v,t}^{s} = N_{v,t} \tag{17}$$
$$N_{v,t} \cdot I_{c,v,t}^{s} P_{c,v}^{\min} \cdot NE_{v}^{s} \le P_{c,v,t}^{s} \le N_{v,t} \cdot I_{c,v,t}^{s} P_{c,v}^{\max} \cdot NE_{v}^{s} \tag{18}$$
$$N_{v,t} \cdot I_{dc,v,t}^{s} P_{dc,v}^{\min} \cdot NE_{v}^{s} \le P_{dc,v,t}^{s} \le N_{v,t} \cdot I_{dc,v,t}^{s} P_{dc,v}^{\max} \cdot NE_{v}^{s} \tag{19}$$
$$E_{v,t}^{s} = E_{v,t-1}^{s} - E_{v,t}^{net,s} - (1 - N_{v,t}) \cdot DR_{v,t}^{s} \cdot NE_{v}^{s} \tag{20}$$
$$E_{v}^{\min} \cdot NE_{v}^{s} \le E_{v,t}^{s} \le E_{v}^{\max} \cdot NE_{v}^{s} \tag{21}$$
$$E_{v,0}^{s} = E_{v,NT}^{s} = E_{v0} \cdot NE_{v}^{s} \tag{22}$$
$$P_{v,t}^{s} = P_{dc,v,t}^{s} - P_{c,v,t}^{s} \tag{23}$$
$$P_{v,\hat{T}}^{s} = E_{v}^{\max} \cdot NE_{v}^{s} \tag{24}$$
$$-\Delta_{i,t}^{\max} \le P_{i,t}^{s} - UX_{i,t}^{s} \cdot P_{i,t} \le \Delta_{i,t}^{\max}$$
$$P_{i}^{\min} \cdot UX_{i,t}^{s} \cdot I_{i,t} \le P_{i,t}^{s} \le P_{i}^{\max} \cdot UX_{i,t}^{s} \cdot I_{i,t} \tag{25}$$
$$\sum_{i \in B_{b}^{i}} P_{i,t}^{s} + \sum_{w \in B_{b}^{w}} P_{w,t}^{s} + \sum_{v \in B_{b,t}^{v}} P_{v,t}^{s} + \sum_{k \in B_{b}^{k}} P_{k,t}^{s} = \sum_{d \in D_{b}} P_{D,t}^{d,s} + \sum_{l \in L_{f,b}} PL_{l,t}^{s} - \sum_{l \in L_{t,b}} PL_{l,t}^{s} \tag{26}$$
$$-M \cdot \left(1 - UY_{l,t}^{s}\right) \le PL_{l,t}^{s} - \frac{\left(\theta_{j,t}^{s} - \theta_{o,t}^{s}\right)}{X_{jo}} \le M \cdot \left(1 - UY_{l,t}^{s}\right) \tag{27}$$
$$-PL_{l}^{\max} UY_{l,t}^{s} \le PL_{l,t}^{s} \le PL_{l}^{\max} UY_{l,t}^{s}. \tag{28}$$

Considering the grid complexity along with the stochastic nature and the mobility of V2G, the proposed optimization problem in (1)–(28) represents a large-scale, nonconvex, nondeterministic polynomial-time hard (NP-hard) problem [26].

The solution to the original problem in such cases would be an intractable task without decomposition. The problem is decomposed into a master MIP problem and several linear programming (LP) subproblems. After the master problem is solved, the subproblems check the network constraints in the base case and all scenarios. Network evaluations for the base case and all scenarios are independent which can be optimized in parallel. Benders cuts are generated and fed back to the master problem to mitigate any violation encountered in the base case or any scenario. The decomposition and respective formulation is shown in Fig. 1.

III. Case Studies

In this section, a 6-bus power system and the 118-bus power system are studied to demonstrate the effectiveness of the proposed approach for analyzing the impact of aggregated PEVs on operation cost, wind curtailment, and optimal unit commitment and dispatch of generation facilities including thermal, hydro, and wind units along with PEV fleets.

A. 6-Bus Power System

A 6-bus power system shown in Fig. 2 is considered to study the integration of PEVs into the power grid. Generators and transmission line data are shown in Tables I and II, respectively. PEVs in various locations are categorized into different fleets based on their driving characteristics. The available energy, max/min capacity and charge/discharge power of individual vehicles are aggregated in PEV fleet characteristics representing max/min capacities, SOC, and max/min charging/discharging capabilities.Tables III and IV show five fleets in the power system. The charging efficiency of a fleet is 85% which is the ratio of energy stored in the battery to the energy drawn from the grid.

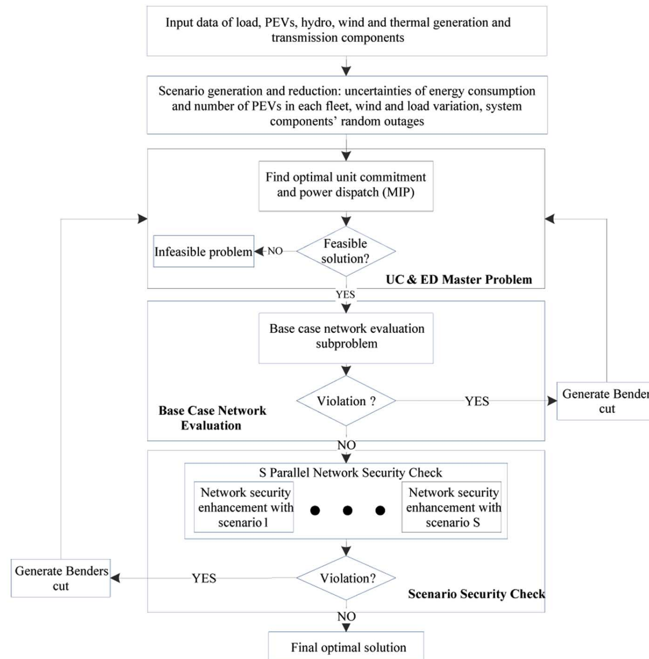

Fig. 1. Proposed Stochastic SCUC with PEV integration in power systems.

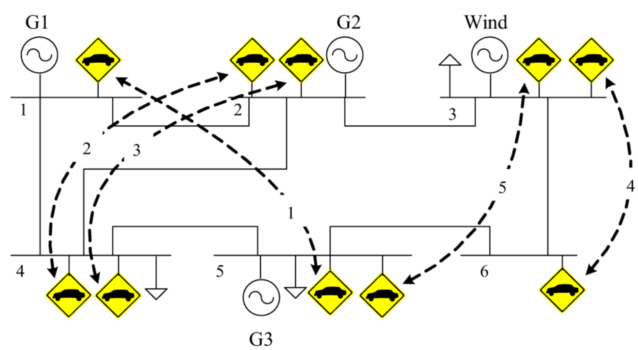

Fig. 2. 6-Bus power system.

TABLE I
Thermal Unit Characteristics

Unit	a ($/MW²)	b ($/MW)	c ($/h)	$P_{\min}$ (MW)	$P_{\max}$ (MW)	SU ($)	SD ($)	Min. Up (h)	Min Dn. (h)
G1	0.099	6.589	211.4	100	320	100	50	4	3
G2	0.203	7.629	217.4	10	160	200	40	3	2
G3	0.494	10.07	102.8	10	100	80	10	1	1

TABLE II
TRANSMISSION LINE CHARACTERISTICS

Line ID	From Bus	To Bus	Impedance (p.u)	Capacity (MW)
1	1	2	0.170	65
2	1	4	0.258	70
3	2	4	0.197	40
4	5	6	0.140	40
5	3	6	0.018	75
6	2	3	0.037	80
7	4	5	0.037	65

TABLE III
PEV FLEET CHARACTERISTICS

PEV fleet No.	Min Cap. (MWh)	Max Cap. (MWh)	Min Charge/ Discharge (kW)	Max Charge/ Discharge (MW)	a ($/MW^2)	b ($/MW)	c ($/h)
1	13.152	65.76	7.3/6.2	24.8/21.08	0.17	8.21	0
2	10.96	54.8	7.3/6.2	14.58/12.4	0.20	8.21	0
3	5.48	27.4	7.3/6.2	7.29/6.2	0.41	8.21	0
4	8.768	43.84	7.3/6.2	11.67/9.92	0.25	8.21	0
5	10.96	54.8	7.3/6.2	14.58/12.4	0.20	8.21	0

TABLE IV
PEV FLEET TRAVEL CHARACTERISTICS

PEV fleet No.	Number of PEVs	First Trip				Second Trip			
		Departure		Arrival		Departure		Arrival	
		Time	Bus	Time	Bus	Time	Bus	Time	Bus
1	3,400	6:00	5	8:00	1	17:00	1	19:00	5
2	2,000	7:00	4	8:00	2	16:00	2	17:00	4
3	1,000	5:00	4	7:00	2	16:00	2	18:00	4
4	1,600	5:00	6	6:00	3	17:00	3	18:00	6
5	2,000	7:00	5	9:00	3	18:00	3	20:00	5

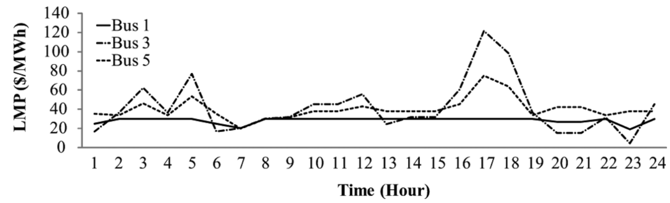

Fig. 3. LMPs in Case 1.

TABLE V
POWER DISPATCH OF PEVS IN GRID CONTROLLED SCHEME (MW)

Fleet	Hours (1-12)											
1	0	0	0	0	0.72	0	0	-0.01	0	0	0	-5.9
2	-7.0	0	0	0	0	-0.47	0	-12.9	-7.98	0	0	0
3	0	0	0	0	0	0	-7.29	-3.29	0	0	0	0
4	0	-0.99	1.96	-0.96	0	-11.6	-11.6	-10.3	0	0	0	5.49
5	0	0	0	0	0	0	0	0	-11.2	0	0	0
Fleet	Hours (13-24)											
1	0	-15.4	0	-15.4	0	0	0	0	0	0	0	0
2	-12.9	0	0	0	12.4	7.50	0	0	0	0	-3.25	0
3	-6.45	0	0	0	0	5.48	0	0	0	0	0	0
4	-11.6	0	-2.39	3.86	0	9.92	-0.08	2.14	3.57	-1.71	2.40	0
5	-14.6	-11.8	-10.9	10.9	12.4	0	0	0	0	0	0	0

TABLE VI
COMMITMENT STATUS IN GRID CONTROLLED SCHEME OF CASE 1

Unit	Hours (1-24)																							
G1	1	1	1	1	1	1	1	1	1	1	1	1	1	1	1	1	1	1	1	1	1	1	1	1
G2	1	1	1	1	1	1	1	1	1	1	1	1	1	1	1	1	1	1	1	1	1	1	1	1
G3	0	0	0	0	0	0	1	1	1	1	1	1	1	1	1	1	1	1	1	1	1	1	1	1

The PEV fleets have different energy requirements. The annual driving distance by a PEV fleet is 12 000 miles with a 32.88 miles average per day [10], [27]. The energy required by a PEV is 9 kWh/day with an average 3.65 miles/kWh [9]. So, the hourly energy required by the fleets is 7.65, 9.00, 2.25, 7.20, and 4.50 MWh, respectively. We assume the required energy for driving in one direction is the same as that of returning to the starting point. The installed wind capacity is 75 MW, which is about 30% of the system peak load with an hourly average wind generation of 11.7%.

We consider two modes of operation. In the grid-controlled mode, PEV charge/discharge decisions are made by power system operators based on the system operation and driving requirements. In the consumer-controlled scheme, SOCs at certain hours are adjusted to represent consumer charging/discharging requirements. The following four cases are considered to evaluate the impact of PEVs on the optimal operation of power systems:

Case 1: Deterministic Solution—Grid-Controlled mode;
Case 2: Deterministic Solution—Consumer-Controlled mode;
Case 3: Stochastic Solution—Grid-Controlled mode;
Case 4: Stochastic Solution—Consumer-Controlled mode.

Case 1: Deterministic Solution-Grid-Controlled Mode

The system load, wind generation, and driving requirements are the same as forecasts. The operation cost is $115 541.36 and the wind curtailment is 0 MWh. Table V shows the charge/discharge mode of PEV fleets in which the aggregated V2G enables a cheaper energy delivery at peak hours. In Table V, the first fleet at bus 5 will inject power to the grid at hour 5 when the bus LMP is higher. The fleet will charge PEV at bus 1 rather than bus 5. Likewise, the fifth fleet will not charge/discharge when connected to bus 5 as both the lowest and the highest LMPs occur on bus 3. In Fig. 3 the maximum LMP is 121.6 $/MWh at bus 3. The LMPs at buses 3 and 5 are higher at hours 3, 5, and 16–18. The fourth and fifth fleets in Table V are discharged at hours 16, and 16–17, respectively, to take advantage of higher LMPs on bus 3.Table VI shows the hourly commitment of generators in which the third generator is not committed for the first six hours in the morning.

The grid operation cost and wind curtailment will increase to $117 424.15 and 1.2 MWh, respectively, if the aggregated PEVs are stationary, i.e., always connected to the same bus. These quantities will decrease when PEVs are mobile in the grid. The mobility of PEVs could enhance the optimal generation while satisfying the fleet requirements. However, constraints imposed by consumers on the energy required for driving a vehicle, maximum storage capacity, and SOC could limit the optimal grid operation. For example, the fourth fleet departs bus 6 in the morning with an SOC of 36.4% and returns in the evening with an SOC of 74.8%. This indicates that the energy is transferred from bus 3 to bus 6 via the fourth fleet.

PEVs may reduce the operation cost by storing energy in one bus without transferring the energy elsewhere. The SOC of the fifth fleet when departing and returning to bus 5 is 36.4%, and the power exchange occurs when the PEV is connected to bus 3. Fig. 4 shows the generation dispatch in which the standard deviation of generation dispatch for Generators 1–3 is 16.1, 10.8, and 11.2 MW, respectively.

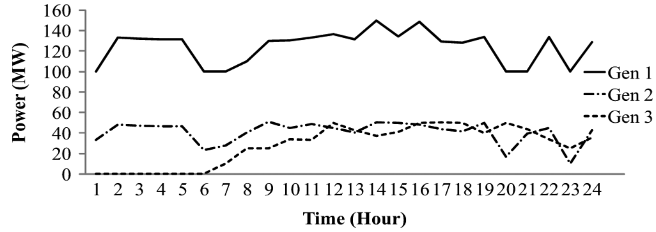

Fig. 4. Hourly dispatch of generators in Case 1.

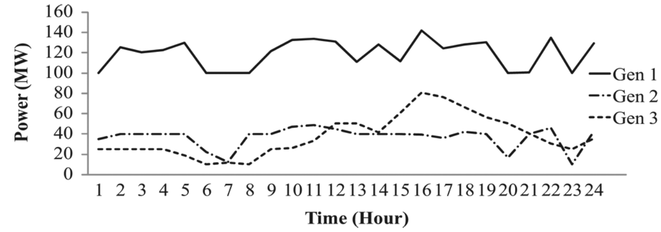

Fig. 5. Hourly dispatch in consumer-controlled scheme in Case 2.

TABLE VII
HOURLY POWER DISPATCH OF PEVS IN CASE 2 (MW)

Fleet	Hours (1-12)											
1	-8.23	0	0	0	-9.76	0	0	-1.72	-0.01	0	0	0
2	-9.59	0	0	0	0	-12.3	0	0	0	0	0	0
3	-5.29	0	0	0	0	0	-5.29	0	0	0	0	0
4	0	-10.3	-4.33	-10.3	0	-8.47	0	0	0	1.93	0	5.49
5	-10.6	0	0	0	0	-0.01	0	0	0	1.96	0	0
Fleet	Hours (13-24)											
1	0	0	-0.81	-15.4	0	0	0	0	0	0	0	0
2	-10.6	0	0	0	12.4	0	0	0	0	0	-3.25	0
3	0	0	0	0	0	0	0	0	0	0	0	0
4	-8.73	0	0	0	0	6.68	-2.93	2.14	5.282	0	2.403	0
5	-12.9	0	0	0	0	0	0	0	0	0	0	0

TABLE VIII
HOURLY COMMITMENT IN CONSUMER CONTROLLED SCHEME OF CASE 2

Unit	Hours (1-24)
G1	1 1 1 1 1 1 1 1 1 1 1 1 1 1 1 1 1 1 1 1 1 1 1 1
G2	1 1 1 1 1 1 1 1 1 1 1 1 1 1 1 1 1 1 1 1 1 1 1 1
G3	1 1 1 1 1 1 1 1 1 1 1 1 1 1 1 1 1 1 1 1 1 1 1 1

TABLE IX
MAXIMUM LMPS ($/MWH)

Bus	Case 1	Case 2
1	30.0	30.0
2	32.0	32.0
3	121.6	336.0
4	64.1	137.9
5	75.0	175.5
6	116.3	317.7

Case 2: Deterministic Solution—Consumer-Controlled Mode

The grid operation cost increases to $119 084.33 as the consumer-controlled mode imposes further constraints on charge/discharge of PEVs.Table VII shows the dispatch of PEV fleets. The wind curtailment is 0 MWh. Comparing Tables VII and V, it is clear that the required SOC at the departure time will cause the fleet to draw more energy from the grid. Unlike Case 1, the fifth fleet at bus 5 is charged at hours 1 and 6 to set the desired SOC at the departure time. Table VIII shows the hourly commitment of thermal generators in which G3 is committed at additional hours as compared to Case 1. Table IX shows a higher LMP and congestion at peak hours in the consumer-controlled scheme.

Fig. 5 shows the generation dispatch profile in which the standard deviations of generation dispatch for Generators 1–3 are 14, 10.4, and 20 MW, respectively. So the generation profile of the most expensive generator (Gen. 3) in Case 1 is smoother than that in Case 2. Hence, a flexible PEV control can reduce the volatility when integrating renewable resources into the grid.

TABLE X
TRANSMISSION LINE CHARACTERISTICS IN CASES 3 AND 4

Line ID	From Bus	To Bus	Capacity(MW)	FOR
1	1	2	97	1%
2	1	4	100	1%
3	2	4	113	1%
4	5	6	81	1%
5	3	6	121	1%
6	2	3	111	1%
7	4	5	103	1%

The generation dispatch volatility could increase the grid operation cost due to turbine wear and tear.

Case 3: Stochastic Solution—Grid-Controlled Mode

In this case, load and wind forecast errors, generation and transmission outages, and the number of PEVs in a fleet and their energy requirements are considered random. The load forecast error follows a normal distribution with a mean value equal to the forecasted load and standard deviation of 5% of the mean value. The forecast error of energy consumption for driving and the number of PEVs in a fleet follow a normal distribution with mean values equal to the forecast as shown in Tables III and IV, and the standard deviationof 5% and 20% of the mean values, respectively. The wind generation forecast is procured based on the typical wind power curve and generated wind speed data. The mean daily wind speed is 10 m/s, which follows a Weibull distribution function with Weibull coefficient equal to 2.1.

The deterministic solution applied to the proposed stochastic model would result in the operation cost and the expected demand mismatch penalty of $129 184.989 and $25 146, respectively. While in the stochastic solution, the operation cost and demand mismatch penalty are $128 174.713 and $20 913, respectively. Hence, the stochastic solution would lower the operating cost by $5243.276 (i.e., $129\,184.989 + 25\,146 - 128\,174.713 - 20\,913$), which is the value of stochastic programming.

In Table X, a case with higher transmission line capacities is considered to avoid any demand mismatch due to transmission congestions. In this case, the grid operation cost in the base case is $113 454.555 and the availability cost of the system is $1789.359, while the wind curtailment in the base case and the expected wind curtailment in scenarios are 117.32 MWh and 40.762 MWh, respectively. Table XI shows the hourly commitment of thermal units in which the third unit is not committed for 10 hours.

Case 4: Stochastic Solution—Consumer-Controlled Mode

Like Case 2, the consumers set the SOC of PEVs prior to departure. In this case, the base case operation cost and availability cost are $114 498.69 and $2108 while the wind curtailment in the base case and the expected wind curtailment in scenarios are 121.097 MWh and 40.816 MWh, respectively. Here, the base case operation cost, availability cost and wind curtailment are

TABLE XI
HOURLY COMMITMENT IN CASE 3

Unit	Hours (1-24)
G1	1 1 1 1 1 1 1 1 1 1 1 1 1 1 1 1 1 1 1 1 1 1 1 1
G2	1 1 1 1 1 1 1 1 1 1 1 1 1 1 1 1 1 1 1 1 1 1 1 1
G3	0 0 0 0 0 0 0 0 0 0 0 1 1 1 1 1 1 1 1 1 1 1 1 1

TABLE XII
HOURLY COMMITMENT IN CASE 4

Unit	Hours (1-24)
G1	1 1 1 1 1 1 1 1 1 1 1 1 1 1 1 1 1 1 1 1 1 1 1 1
G2	1 1 1 1 1 1 1 1 1 1 1 1 1 1 1 1 1 1 1 1 1 1 1 1
G3	0 0 0 0 0 1 0 0 0 1 1 1 1 1 1 1 1 1 1 1 1 1 1 1

TABLE XIII
WIND SPEED PROFILE AT SITES

	site 1	site 2	site 3	site 4	site 5
Weibull Coefficient	1.17	2.03	2.19	2.9	2.26
Auto Correlation Factor	0.761	0.943	0.957	0.88	0.928
Diurnal Wind Pattern	0.11	0.0944	0.0969	0.0196	0.0668
Hour of Peak Wind Speed	24	14	13	20	22

TABLE XIV
PEV FLEET CHARACTERISTICS

PEV Fleet	Min Energy (MWh)	Max Energy (MWh)	Charge/Discharge Min (kW)	Charge/Discharge Max (MW)	a ($/MW^2)	B ($/MW)	c ($/h)
1	131.52	986.4	7.3/6.2	248/210.8	0.57	27.35	0
2	109.6	822	7.3/6.2	145.8/124	0.68	27.35	0
3	54.8	411	7.3/6.2	72.9/62	1.36	27.35	0
4	87.68	657.6	7.3/6.2	116.7/99.2	0.85	27.35	0
5	109.6	822	7.3/6.2	145.8/124	0.68	27.35	0

TABLE XV
RESULTS FOR FOUR CASES (BASE CASE)

Case	Cost ($)	Wind Curtailment (MWh)
1	1,323,982	305.456
2	1,327,672	348.572
3	1,352,637	178.216
4	1,357,843	169.145

increased as compared to those in Case 3. Table XII shows the hourly commitment of generators in Case 3. The hourly commitment of G3 is increased by two hours in this case.

B. 118-Bus Power System

In this case, the modified IEEE 118-bus system shown in http://motor.ece.iit.edu/EV/118.emf is considered. Five 150 MW wind generation sites are considered on buses 12, 31, 66, 72, and 100, respectively. Table XIII shows the intermittent wind speed information. A total of 100 000 PEVs are divided into 5 fleets based on their driving patterns. The PEVs in fleets are 34 000, 20 000, 10 000, 16 000, and 20 000, respectively. Table XIV shows the fleet characteristics. The fleet travel schedules are similar to those in the previous case study. The same four cases discussed in the 6-bus system are considered.

Table XV shows the optimal base case cost and wind curtailment in each case. Table XVI shows the expected wind curtailment and the availability cost in Cases 3 and 4. In the grid-controlled scheme, the expected wind curtailment and availability cost are lower. Table XVII shows the operation cost. Comparing Cases 3 and 4, the operation costs are higher in the consumer-controlled scheme because of introducing additional

TABLE XVI
EXPECTED SCENARIO RESULTS FOR CASES 3 AND 4

Case	Avail. Cost ($)	Exp. Wind Curtail (MWh)
3	12,649.754	328.57
4	14,289.818	367.28

TABLE XVII
SCENARIO COSTS IN CASES 3 AND 4 ($)

Scenario	Case 3	Case 4
1	1,371,254	1,378,357
2	1,457,163	1,466,943
3	1,408,596	1,414,523
4	1,369,053	1,374,058
5	1,413,558	1,414,729
6	1,423,133	1,427,015
7	1,428,505	1,429,073
8	1,374,482	1,378,838
9	1,411,435	1,415,783
10	1,444,603	1,444,894
11	1,397,722	1,401,078
12	1,408,407	1,419,582

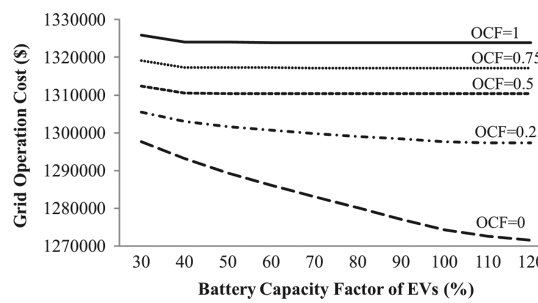

Fig. 6. Grid operation cost in a grid-controlled scheme.

constraints. The results are consistent with that in the previous case study.The solution time in this case is about 58 h on a 3.6 GHz personal computer with CPLEX 12.1. Parallel processing of a larger server with multiple CPUs or several large servers could reduce the computation time. In addition, practical considerations for the implementation of PEV in a specific power system could introduce additional short cuts for reducing the computation time. The grid operation cost will decrease with larger size PEV storage. However, the primary goal of PEV fleets is transportation rather than the provision of ancillary services in power grids.

Fig. 6 shows the relationship between the PEV storage capacity, the charging/discharging cost, and the grid operation cost. The battery capacity factor shows the size of the battery as a percentage of a nominal battery capacity. The operation cost factor (OCF) shows the charging/discharging cost as a percentage of nominal cost for battery operation. In Fig. 6, grid operation cost decreases as OCF is reduced. Also, the grid operation cost decreases as PEV battery capacity factor increases. Unlike the grid-controlled scheme, the increase in PEV storage capacity may not reduce the grid operation cost in the consumer-controlled scheme. The SOC constraints may restrict the V2G reduction of the grid operation cost. Fig. 6 shows that the increase in PEV charging/discharging costs will restrict the PEV storage participation to the operation cost reduction. The PEV contribution to the operation cost reduction may not be significant in an unconstrained (no transmission congestion) power system and system operators may consider dispatching more expensive units rather than using PEV fleets as storage.

IV. Discussions

The integration of PEVs will introduce distributed and mobile demands and storage in power systems. The mobility of PEV fleets will impose additional operation constraints and introduce benefits for supplying critical power system loads in specific locations and periods. The variability of renewable generation resources may also be managed properly by charging/discharging capability of mobile PEV fleets.

Once PEVs are connected to the grid, they can draw energy, store it in batteries, and inject it back to the grid at other times and locations in order to decrease grid operation costs. Once in the V2G mode, PEVs can transfer energy between locations and contribute to the provision of ancillary services and congestion mitigation in transmission systems. Hence, V2G can help ISOs lower grid operation costs by taking advantage of the fact that the stored energy in PEVs can be transmitted between locations without obeying power flow rules.

However, PEV utilization in power systems could introduce additional obstacles and limitations. One issue is that the cost of storing and delivering energy by PEV for reducing power system operation costs may not be much cheaper than that of energy supplied by the grid. The higher charging/discharging cycles may reduce the battery life and impose further limitations on PEV operations as a vehicle. Moreover, PEV storage requirements as a vehicle could impose further restrictions on the grid utilization of PEV storage. Another challenge is the availability of PEV at certain hours and locations as storage when PEV is mobile. The driving patterns and the number of vehicles in each fleet can alter the characteristics of ancillary services provided by PEV fleets. However, the transmission congestion cost over an extended period could far exceed the PEV storage cost.

V. Conclusions

In this paper, the impact of integrating PEV fleets into power systems is evaluated. The proposed stochastic model incorporates the modeling of PEV fleets according to the power system and PEV fleet constraints and requirements. The contributions of the paper include:

- The PEV fleet modeling in power systems is considered using the MIP formulation.
- The detailed power transmission system modeling and transmission constraints are included in the model.
- The integration of high penetration of renewable generation resources in power systems is considered.
- The uncertainties imposed by PEV fleets, renewable energy resources, and transmission and generation components are included.
- The operation schemes of PEV fleets and their impacts on power system operations are considered.
- The impact of PEV on thermal generation profile in power systems is evaluated.

It is shown that the PEV mobility can efficiently transfer energy throughout the network. PEVs can also help reduce the grid operation cost by providing energy storage for renewable energy resources. The PEV charging/discharging costs, limited storage capacity, required energy for driving PEV, and the SOC constraints imposed by consumers will further restrict the reduction in grid operation costs. When consumers set the SOC of PEVs, the grid operation costs will increase and PEV capabilities for transferring energy between locations will be limited.

References

[1] "Reducing greenhouse gas emissions from U.S. transportation," [Online]. Available: www.pewclimate.org/docUploads/ustransp.pdf

[2] H. Lund and W. Kempton, "Integration of renewable energy into the transport and electricity sectors through V2G," *Energy Policy*, vol. 36, no. 9, pp. 3578–3587, Sep. 2008.

[3] "Global wind 2008 report," Global Wind Energy Council (GWEC) [Online]. Available: http://www.gwec.net/fileadmin/documents/Global%20Wind%202008%20Report.pdf

[4] B. C. Ummels, E. Pelgrum, and W. L. Kling, "Integration of large-scale wind power and use of energy storage in the Netherlands' electricity supply," *IET Renewable Power Gener.*, vol. 2, no. 1, pp. 34–46, Mar. 2008.

[5] M. Lu, C. Chang, W. Lee, and L. Wang, "Combining the wind power generation system with energy storage equipment," *IEEE Trans. Ind. Appl.*, vol. 45, no. 6, pp. 2109–2115, Nov. 2009.

[6] Y. Lee, A. Khaligh, and A. Emadi, "Advanced integrated bi-directional AC/DC and DC/DC converter for plug-in hybrid electric vehicles," *IEEE Trans. Veh. Technol.*, vol. 58, no. 8, pp. 3970–3980, Oct. 2009.

[7] S. S. Raghavan, O. C. Onar, and A. Khaligh, "Power electronic interfaces for future plug-in transportation systems," *IEEE Power Electron. Soc. Newslett.*, vol. 24, no. 3, pp. 23–26, Jul. 2010.

[8] S. M. Lukic, J. Cao, R. C. Bansal, R. Rodriguez, and A. Emadi, "Energy storage systems for automotive applications," *IEEE Trans. Ind. Electron.*, vol. 55, no. 6, pp. 2258–2267, Jun. 2008.

[9] J. Tomic and W. Kempton, "Using fleets of electric-drive vehicles for grid support," *J. Power Sources*, vol. 168, no. 2, pp. 459–468, Jun. 2007.

[10] A. Saber and G. Venayagamoorthy, "Plug-in vehicles and renewable energy sources for cost and emission reduction," *IEEE Trans. Ind. Electron.*, unpublished.

[11] W. Kempton and J. Tomic, "Vehicle to gird power implementation: From stabilizing the grid to supporting large-scale renewable energy," *J. Power Sources*, vol. 144, no. 1, pp. 280–294, Apr. 2005.

[12] W. Kempton and J. Tomic, "Vehicle-to-grid power fundamentals: Calculating capacity and net revenue," *J. Power Sources*, vol. 144, no. 1, pp. 268–279, Jun. 2005.

[13] M. Korpas, R. Hildrum, and A. T. Holen, "Operation and sizing of energy storage for wind power plants in a market system," in *Proc. 14th PSCC*, Sevilla, Spain, Jun. 2002.

[14] E. D. Castronuovo and J. A. P. Lopes, "Wind and small-hydro generation. an optimization approach for daily integrated operation," in *Proc. 2003 EWEA*, Madrid, Spain, Jun. 2003.

[15] E. D. Castronuovo and J. A. P. Lopes, "On the optimization of the daily operation of a wind-hydro power plant," *IEEE Trans. Power Syst.*, vol. 19, no. 3, pp. 1599–1606, Aug. 2004.

[16] E. D. Castronuovo and J. A. P. Lopes, "Bounding active power generation of a wind-hydro power plant," in *Proc. Int. Conf. Probab. Methods Appl. Power Syst.*, Sep. 2004, pp. 705–710.

[17] R. Billinton and R. Allan, *Reliability Evaluation of Power Systems*, 2nd ed. London, U.K.: Plenum, 1996.

[18] W. H. Greene, *Econometric Analysis*, 5th ed. Upper Saddle River, NJ: Prentice-Hall, 2003.

[19] J. F. Manwell, J. G. McGowan, and A. L. Rogers, *Wind Energy Explained*. New York: Wiley, 2002.

[20] J. Dupacová, N. Gröwe-Kuska, and W. Römisch, "Scenario reduction in stochastic programming: An approach using probability metrics," *Math. Program. A*, vol. A 95, pp. 493–511, 2003.

[21] GAMS/SCENRED Documentation [Online]. Available: http://www.gams.com/docs/document.htm

[22] D. Gan and E. Litvinov, "Energy and reserve market design with explicit consideration to lost opportunity costs," *IEEE Trans. Power Syst.*, vol. 18, no. 1, pp. 53–59, Feb. 2003.

[23] L. Wu, M. Shahidehpour, and T. Li, "Stochastic security-constrained unit commitment," *IEEE Trans. Power Syst.*, vol. 22, no. 2, pp. 800–811, May 2007.

[24] T. Li and M. Shahidehpour, "Price-based unit commitment: A case of lagrangian relaxation versus mixed integer programming," *IEEE Trans. Power Syst.*, vol. 20, no. 4, pp. 2015–2025, Nov. 2005.

[25] L. Wu, "A tighter piecewise linear approximation of quadratic cost curves for unit commitment problems," *IEEE Trans. Power Syst.*, vol. 26, no. 4, pp. 2581–2583, 2011.

[26] X. Guan, Q. Zhai, and A. Papalexopoulos, "Optimization based methods for unit commitment: Lagrangian relaxation versus general mixed integer programming," in *Proc. IEEE Power Eng. Soc. Meet.*, Jul. 2003, vol. 2.

[27] C. Roe, A. P. Meliopoulos, J. Meisel, and T. Overbye, "Power system level impacts of plug-in hybrid electric vehicles using simulation data," in *Proc. IEEE Energy 2030*, Atlanta, GA, Nov. 17–18, 2008.

Mohammad E. Khodayar (S'09) received the B.S. degree in electrical engineering from Amirkabir University of Technology (Tehran Polytechnic), Iran, and the M.S. degree in electrical engineering from the Sharif University of Technology, Iran. Presently he is working toward the Ph.D. degree in electrical engineering at the Illinois Institute of Technology, Chicago.

Lei Wu (M'07) received the B.S. degree in electrical engineering and the M.S. degree in systems engineering from Xi'an Jiaotong University, China, in 2001 and 2004, respectively, and the Ph.D. degree in EE from the Illinois Institute of Technology, Chicago, in 2008.

Presently, he is an Assistant Professor in the ECE Department at Clarkson University, Potsdam, NY. His research interests include power systems restructuring and reliability.

Mohammad Shahidehpour (F'01) is the Bodine Professor and Director of the Robert W. Galvin Center for Electricity Innovation at the Illinois Institute of Technology, Chicago. He is an Honorary Professor in the King Abdulaziz University in Saudi Arabia, North China Electric Power University, and the Sharif University of Technology in Iran.